Available online at www.sciencedirect.com
ScienceDirect

Catalysis Today 120 (2007) 174–181

CATALYSIS TODAY

www.elsevier.com/locate/cattod

CdS–$AgGaS_2$ photocatalytic diodes for hydrogen production from aqueous Na_2S/Na_2SO_3 electrolyte solution under visible light ($\lambda \geq 420$ nm)

Jum Suk Jang [a], Dong Won Hwang [b], Jae Sung Lee [a,*]

[a] *Department of Chemical Engineering, School of Environmental Engineering,*
Pohang University of Science and Technology (POSTECH), San 31 Hyoja-dong, Pohang 790-784, Republic of Korea
[b] *Manufacturing Technology Team, Semiconductor Business, Samsung Electronics Co. Ltd.,*
San #16, Banwol-dong, Hwangsung 445-701, Republic of Korea

Abstract

A p-type semiconductor, bulky $AgGaS_2$, was prepared by the conventional solid state reaction and heat-treated at various temperatures under He and H_2S gas flow to eliminate vacancies or interstitial defects and to improve the crystallinity. A p–n diode, n-CdS/p-AgGaS2 was fabricated by decorating $AgGaS_2$ surface with nanoparticles of n-type CdS by the hydrothermal treatment. The configuration was confirmed by XRD, UV–vis spectroscopy and TEM. The composite photocatalyst of this new configuration exhibited a high rate of hydrogen production under visible light irradiation ($\lambda \geq 420$ nm) from water containing sulfide and sulfite as hole scavengers. The photocatalytic diode system formed with n- and p-type semiconductors results in efficient charge separation, caused by the rectification of photo-electrons and holes generated upon photo-absorption.

Keywords: $AgGaS_2$; CdS; Photocatalytic diode; Hydrogen production; Photocatalysts

---

1. Introduction

Sunlight is a clean, renewable and abundant energy source and its conversion to hydrogen has been considered an ideal solution to counter the depletion and environmental problems of fossil fuels. Among hydrogen containing sources, H_2S gas is an attractive source because it is more easily converted to hydrogen (relative to water, for example) with a lower energy input, and it is a harmful toxic gas that should be removed anyway [1,2]. Yet, there is still need to develop highly active photocatalysts working under visible light in order to put this technology into practical applications [3–5].

The $AgGaS_2$ is a p-type material of I–III–VI ternary semiconductors, which crystallize in the chalcopyrite structure [6,7]. This material has a direct bandgap of about 2.68 eV and is a promising material for solar cells, non-linear optical devices and blue light emitting diodes (LED) [8–10]. While $AgGaS_2$ can be made as a low-resistivity p-type semiconductor, n-type conductivity appears difficult or impossible to achieve. Thus one can fabricate p–n heterojunctions or heterodiodes employing a compatible n-type semiconductor as ZnS or CdS for LED applications [11–14]. CdS is well known to exhibit a high photocatalytic activity in the presence of sacrificial reagents and it can be made as n-type (but not p-type) [15,16]. The fundamental direct band gap energy of wurtzite CdS is 2.42 eV at 300 K, close to that of $AgGaS_2$ (2.68 eV). Consequently, comparable injection ratios are likely for electrons and holes. It has been demonstrated in photovoltaic cells that diode structures made of n- and p-type semiconductors show greatly enhanced activities compared to devices consisting of a single semiconductor [17]. In photocatalytic systems, p–n heterojunction or heterodiode is also an interesting structure because the formation of p–n composite photocatalyst could lead to an efficient electron-hole separation that minimizes the energy wasteful electron-hole recombination. Recently, we demonstrated a photocatalytic nanodiode (PCD) system of p-$CaFe_2O_4$/n-$PbBi_2Nb_{1.9}W_{0.1}O_9$ that exhibited a very high activity for hydrogen production [18]. Previously, Nojik

---

* Corresponding author. Tel.: +82 54 279 2266; fax: +82 54 279 5528.
E-mail address: jlee@postech.ac.kr (J.S. Lee).

0920-5861/$ – see front matter © 2006 Elsevier B.V. All rights reserved.
doi:10.1016/j.cattod.2006.07.052

constructed an n-TiO_2/p-GaP diode electrode for a photoelectrochemical (PEC) cell that was much more active than either n-TiO_2 or p-GaP single-component electrodes for the decomposition of water [19].

In the present work, we have chosen CdS as the n-type semiconductor and $AgGaS_2$ as the p-type semiconductor to form an exploratory photocatalytic diode. This sulfide-type diode was investigated for hydrogen production under visible light irradiation ($\lambda \geq 420$ nm) from water containing sulfide and sulfite as hole scavengers.

2. Experimental

2.1. Preparation of CdS and $AgGaS_2$ photocatalysts

The nanosized CdS photocatalyst was prepared by a precipitation method followed by hydrothermal treatment. A stoichiometric amount of Na_2S aqueous solution was added drop-by-drop to $Cd(NO_3)_2$ dissolved in isopropyl alcohol. Precipitated suspension was hydrothermally treated in autoclave at 393 K for 3days. After the completion of the reaction, the precipitates were filtered and washed several times with deionized water. Filtered powders were dried at 343 K for 5 h in a convection oven. $AgGaS_2$ (AGS) was prepared by the conventional solid-state reaction. Thus, a stoichiometric mixture of Ag_2S (Aldrich 99.9%) and Ga_2S_3 (10% excess, Aldrich 99.99%) were mixed and ground in a *mortar* in the presence of ethanol and dried in an oven. Pelletized powders were calcined at 1073 K for 5 h under N_2 flow. The obtained powders were ground in a *mortar* in the presence of ethanol. The obtained powders were heat-treated at 873–1123 K for 3 h under He (21 μmol s^{-1}) and H_2S (14 μmol s^{-1}) gas flow to remove defects and increase the crystallinity of $AgGaS_2$.

2.2. Fabrication of CdS/$AgGaS_2$ photocatalytic diode (PCD)

To fabricate CdS/$AgGaS_2$ photocatalytic heterodiode, bulky $AgGaS_2$ was stirred in isopropyl alcohol. Then, a stoichiometric amount of Na_2S aqueous solution was added drop-by-drop while stirring to a solution containing $AgGaS_2$ powder and $Cd(NO_3)_2$ dissolved in isopropyl alcohol (15 wt.% of CdS in CdS/$AgGaS_2$). The prepared composite powder was hydrothermally treated in an autoclave at 393–423 K for 1 day. After completion of the reaction, the precipitates were filtered and washed several times with deionized water. Filtered powders were dried at 343 K for 5 h in a convection oven.

2.3. Characterization

The crystalline phases of the products were determined by X-ray diffractometer (Mac Science Co., M18XHF) with monochromatic Cu Kα radiation at 40 kV and 200 mA. The optical properties were analyzed by UV–vis diffuse reflectance spectrometer (Shimadzu, UV 2401). The morphology of photocatalysts were investigated by the field emission scanning electron microscopy (SEM, Hitachi, S-4200) and a transmission electron microscope (JEOL JEM 2010F, Field Emission Electron Microscope) instrument operated at 200 kV. The bulk composition of the catalysts was determined by an energy dispersive spectrometer (EDS, EDAX Inc., Classic 10L Dewar). Data collection for Reitveld analysis was performed at HRPD Beamline of Pohang light source (PLS) located in Pohang, Korea, and the used software for cell refinement was *FULLPROF2K* [25].

2.4. Photocatalytic reaction

The photocatalytic reaction for hydrogen production was carried out at room temperature under normal pressure in a closed circulation system using a Hg-arc lamp (450 W) equipped with UV cut off filter ($\lambda \geq 420$ nm) placed in an inner irradiation-type pyrex reaction cell. The H_2 evolution was determined in an aqueous solution (100 ml) containing 0.1 g catalyst and 0.1 M Na_2S + 0.02 M Na_2SO_3 as hole scavengers. The evolved amounts of H_2 were determined by gas chromatography (TCD, molecular sieve 5-Å column and Ar carrier). The 1.0 wt.% of Pt metal was loaded as a co-catalyst onto the semiconductor photocatalysts by the photodeposition method.

3. Results and discussion

3.1. Single-component p-type $AgGaS_2$ (AGS) photocatalyst

Bulky $AgGaS_2$ was prepared by the conventional solid-state reaction and calcined at 1073 K under N_2 flow for 5 h. In XRD, most reflections were indexed to the tetragonal phase $AgGaS_2$. The cell constants of this material is known as $a = 5.765$ and $c = 10.281$ Å in the literature [20]. But, there exist extra peaks due to impurity phases. To remove vacancies or interstitial defects and to improve the crystallinity, $AgGaS_2$ was heat-treated at various temperatures under H_2S (40 vol.%) gas flow diluted with He. Fig. 1 shows XRD patterns of the samples heat-treated at various temperatures under H_2S gas flow. The AGS sample calcined at 1073 K for 5 h under N_2 is a starting material and has a tetragonal structure with the space group of $I\bar{4}2d$ as the main structure and impurity components such as Ga_2O_3 and Ag_9GaS_6. Two impurity components were identified by a fit of full-profile structure refinement. When heat-treatment temperature was raised over 1073 K, crystal structure was completely transformed into the tetragonal structure without any impurity component. Thus, the heat-treatment temperature for the preparation of bulk $AgGaS_2$ photocatalyst as p-type material was chosen to be 1123 K.

Full-profile structure refinement of the measured powder diffraction data was performed with *FULLPROF2K* [25]. The observed powder XRD data, represented by black solid line at the top of Fig. 2, corresponded to the tetragonal phase. The result of refinement, as shown in Table 1, shows that the lattice parameters of $AgGaS_2$ are in agreement with that of $AgGaS_2$ previously reported [21].

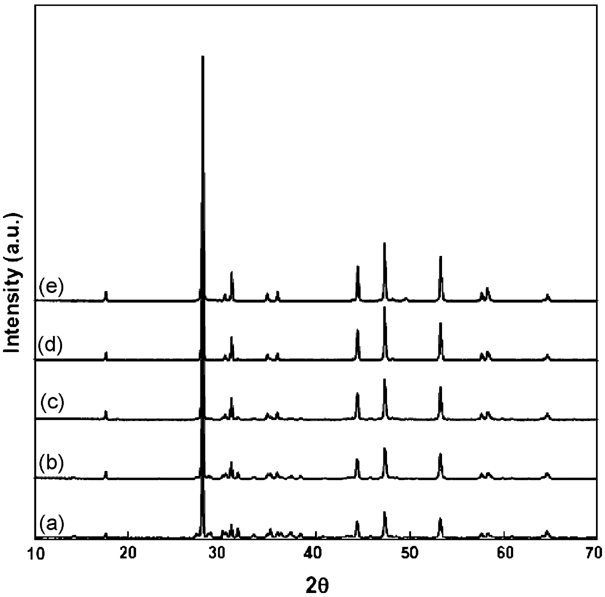

Fig. 1. X-ray diffraction pattern of $AgGaS_2$ not heat-treated (a) and heat-treated at (b) 873 K, (c) 973 K, (d) 1073 K, (e) 1123 K for 5 h under H_2S (14 μmol s^{-1}) and He (21 μmol s^{-1}) gas flow.

Fig. 3 shows the UV-diffuse reflectance (DR) spectra for these samples treated at different temperatures under H_2S flow. The positions of absorption edge were not much different among the samples. The untreated material (a) showed a diffuse absorption region (500–700 nm) due to vacancies or interstitial defects in the chalcopyrite lattice, which caused these compounds to have a poor crystal quality and a poor optical property. But, when this material was heat-treated at high temperatures under H_2S gas flow, the resulting $AgGaS_2$ photocatalyst showed a good absorbance and crystallinity without impurity components.

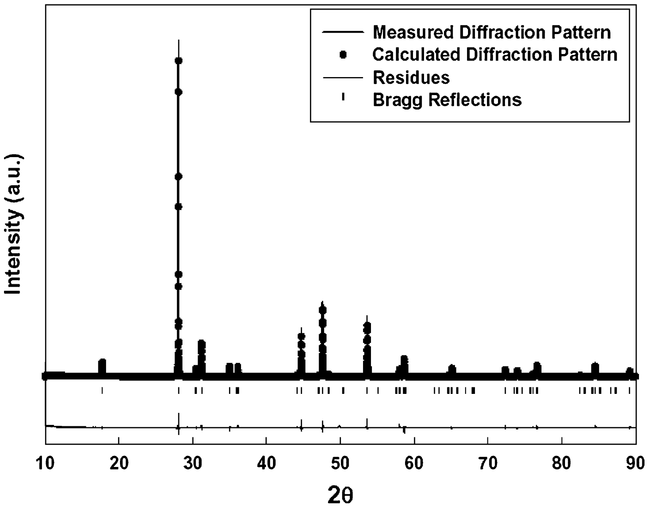

Fig. 2. Observed and calculated X-ray powder diffraction patterns of $AgGaS_2$ (H_2S, 1123 K) are represented on the top by dots and a solid line, respectively. Vertical marks in the middle represent the calculated Bragg reflection angles. The trace on the bottom is a plot of the difference between the observed and calculated intensities.

Table 1
Reitveld refinement of lattice parameters for $AgGaS_2$ heat-treated at 1173 K

Material	$AgGaS_2$
a (Å)	5.759
b (Å)	5.759
c (Å)	10.302
α (°)	90
β (°)	90
γ (°)	90
V (Å^3)	341.68

Full-profile structure refinement of the measured powder diffraction data was performed with *FULLPROF2K*.

The morphology of bulky $AgGaS_2$ particles heat-treated at various temperatures under H_2S gas flow was observed by SEM as shown in Fig. 4. Their morphologies were irregular bulk particles with a particle size of ca. 2–3 μm. In the samples treated at low temperatures, we can observe bulky $AgGaS_2$ particles surrounded by the broken powders having sharp edges. But, there were almost no broken particles in bulky $AgGaS_2$ particles heat-treated at high temperatures with H_2S gas.

Elemental analyses of $AgGaS_2$ before and after heat-treatment at 1123 K for 3 h under H_2S gas flow were made from EDAX data, as shown in Fig. 5(a) and (b). This indicates that after heat-treatment most of oxygen was removed and the composition of this material stayed near stoichiometry. But, the treatment did not remove completely the oxygen on the surface of $AgGaS_2$. Despite the considerable amount of oxygen on the surface of $AgGaS_2$, XRD pattern of $AgGaS_2$ heat-treated at 1123 K showed a clean pattern and a high crystallinity.

Shown in Fig. 6 are the results of photocatalytic hydrogen production from an aqueous electrolyte solution containing 0.1 M Na_2S and 0.02 M Na_2SO_3 as sacrificial reagents under visible light irradiation (using a cut-off filter of $\lambda \geq 420$ nm for

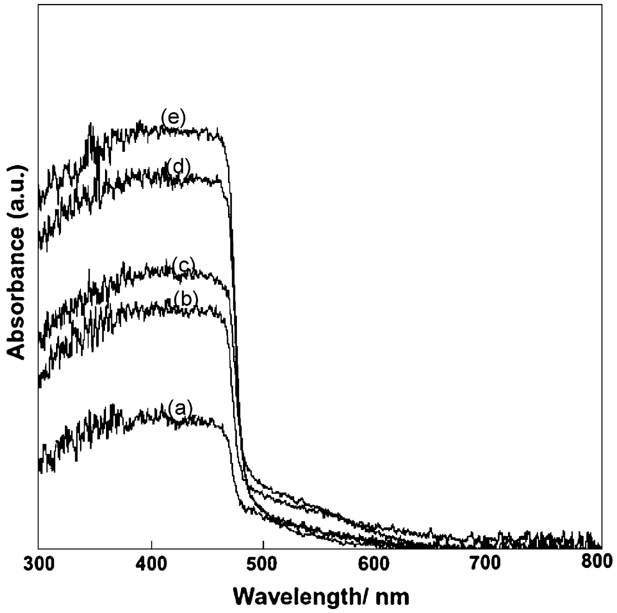

Fig. 3. UV–vis diffuse reflectance spectra of untreated $AgGaS_2$ (a) and $AgGaS_2$ heat-treated at (b) 873 K, (c) 973 K, (d) 1073 K, (e) 1123 K for 3 h under H_2S/He gas flow.

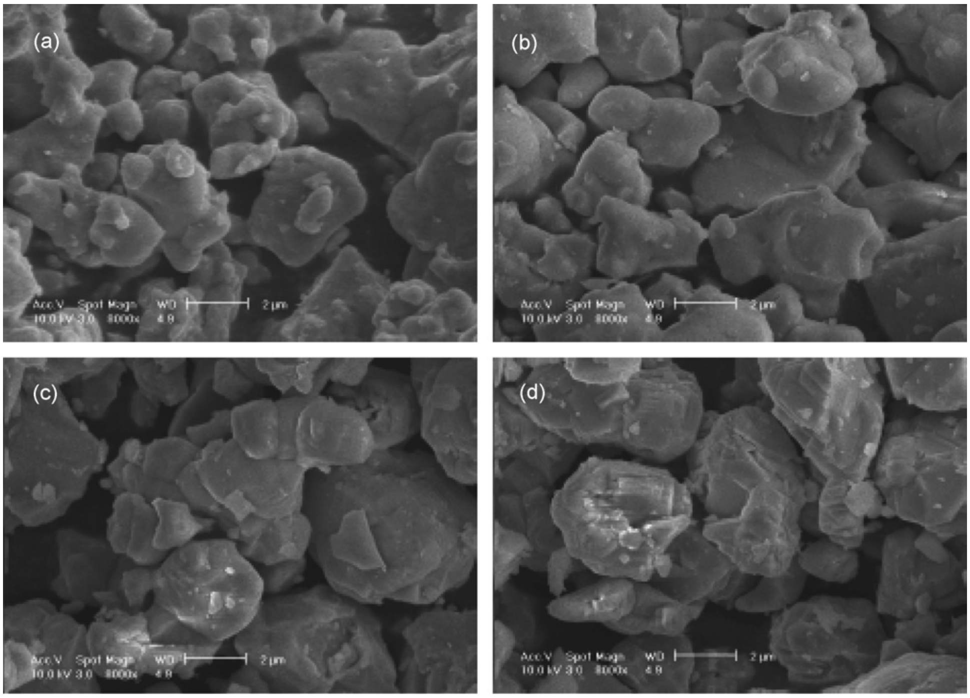

Fig. 4. SEM images of $AgGaS_2$ heat-treated at (a) 873 K, (b) 973 K, (c) 1073 K and (d) 1123 K. All samples were heat-treated under H_2S (14 µmol s^{-1}) and He (21 µmol s^{-1}) gas flow for 3 h.

all catalysts). The rates of hydrogen evolution over $AgGaS_2$ heat-treated at higher temperatures (1073 and 1123 K) were higher than those of photocatalysts untreated and treated at lower temperatures (873 and 973 K). This result can be correlated with XRD patterns and UV-vis DRS. Compared to AGS heated-treated at low temperatures under H_2S gas flow, $AgGaS_2$ heated-treated at high temperatures showed a high crystallinity without any impurity structure and improved absorbance with a sharp edge. From these results, it can be concluded that the impurity level and crystallinity of $AgGaS_2$ are important for the photocatalytic activity.

3.2. CdS/$AgGaS_2$ photocatalytic diode (PCD)

To construct the photocatalytic diode, we need a pair of n- and p-type semiconductors. We have chosen CdS as the n-type semiconductor and $AgGaS_2$ as the p-type semiconductor. The fabrication method of this diode structure is also critical for the photocatalytic activity. In our previous work [22], we have demonstrated that a nano-bulk composite structure is particularly useful, in which nanoparticles of a semiconductor interface with highly crystalline bulky particles of the other semiconductor. Considering the sensitive effect of the crystallinity of $AgGaS_2$ on its photocatalytic activity, we chose to fabricate a photocatalytic diode of bulky $AgGaS_2$ decorated by nanoparticles of CdS by a hydrothermal method as described in Section 2.

Fig. 7 shows X-ray diffraction patterns of (a) CdS treated hydrothermally at 393 K for 1 day, (b) AGS treated under H_2S flow at 1123 K for 3 h, (c) CdS/AGS composite treated hydrothermally at 393 K for 1 day, and (d) CdS/AGS composite treated hydrothermally at 423 K for 1 day. The crystallinity of CdS in CdS/AGS photocatalytic diode (PCD) was as low as the single component CdS nanoparticle as seen from the intensity

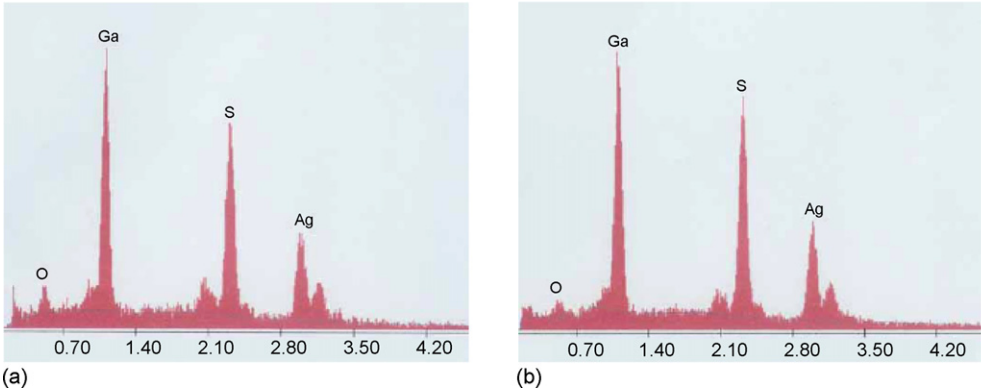

Fig. 5. EDAX spectra of (a) AGS-starting material and (b) AGS heat-treated at 1123 K for 3 h with H_2S/He gas.

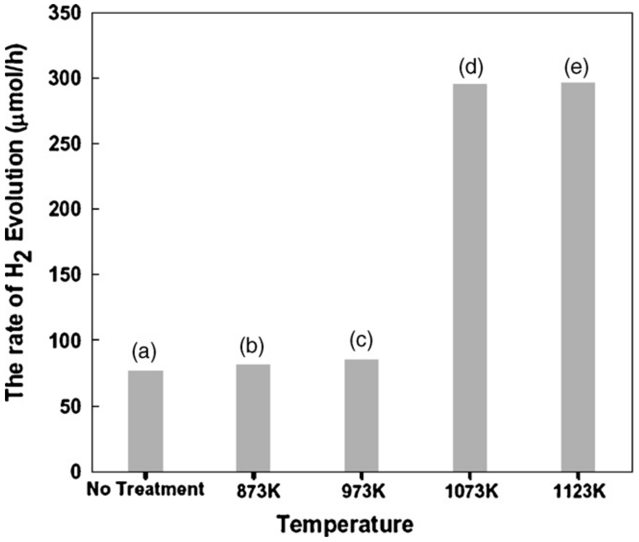

Fig. 6. The rate of photocatalytic hydrogen production at room temperature over of untreated $AgGaS_2$ (a) and $AgGaS_2$ heat-treated at (b) 873 K, (c) 973 K, (d) 1073 K, (e) 1123 K for 3 h under H_2S/He gas flow. Catalysts: 0.1 g loaded with 1 wt.% Pt, electrolyte: 0.1 M Na_2S + 0.02 M Na_2SO_3.

of XRD peaks and considering its concentration (15 wt.%) in the composite. To improve the crystallinity of CdS in PCD, we increased the temperature of hydrothermal treatment (Fig. 7d). In spite of the higher temperature of hydrothermal treatment, the crystallinity of CdS in CdS/AGS photocatalytic diode (PCD) was not clearly revealed and its main peak remained hidden under the peak of $AgGaS_2$ and showed only very small intensity. Hence, there was no distinct difference in XRD patterns of three samples containing $AgGaS_2$. Some extra peaks are observed around 21.8, 33.9 and 37.3° in Fig. 7c and d, which could be assigned to β-$CdSO_4$ (JCPDS 16-0253). This impurity phase seems to originate from superficial oxidation of CdS. The pure CdS showed a mixture of cubic and hexagonal phases and the $AgGaS_2$ phase was a well-developed tetragonal structure both in single and PCD photocatalysts. Thus, each component of PCD maintained its structural identity during the formation of PCD composite.

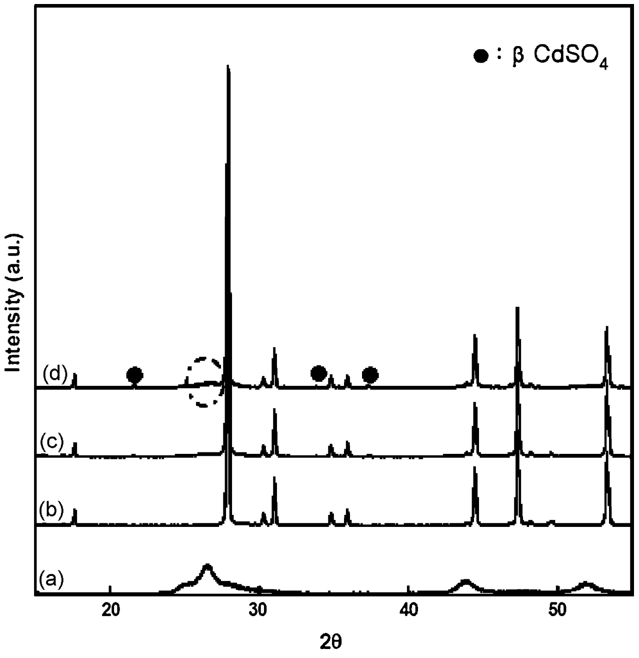

Fig. 7. X-ray diffraction pattern of (a) CdS treated hydrothermally at 393 K for 1 day, (b) AGS treated in H_2S/He at 1123 K for 3 h, (c) CdS/AGS PCD treated hydrothermally at 393 K for 1 day, and (d) CdS/AGS PCD treated hydrothermally at 423 K for 1 day. The low 2θ side of the main peak in (c) and (d) indicates the presence of β-$CdSO_4$ as an impurity phase.

The diffuse reflection spectra for these catalysts are shown in Fig. 8. The AGS photocatalyst showed a sharp edge at 490 nm, while that of CdS was observed at 570 nm. The spectrum of the CdS/AGS composite photocatalyst showed a combination of these two spectra, although CdS in PCD photocatalysts showed a small blue-shift of the main absorbance edge. Although the increased temperature did not lead to any apparent change due to the small peak intensities of CdS in XRD patterns of CdS/AGS composite photocatalysts, CdS in composite photocatalyst hydrothermally treated at higher temperatures showed a small red-shift and sharpness of UV-DR spectra probably due to the enhanced contribution from CdS as shown in Fig. 8d. This is in agreement with the previous report by our group and Kisch et al. that the band gap of CdS employed in composite photocatalyst is shifted by an electronic semiconductor-support interaction (SEMSI) [22–24]. It was confirmed that CdS/AGS photocatalytic diode showed a UV-DR spectrum similar to that of a physically mixed CdS/AGS sample.

Fig. 9 shows electron microscope images of (a) CdS nanoparticles, (b) bulky $AgGaS_2$ heat-treated at 1123 K for 3 h under H_2S gas flow, (c) CdS/AGS diode structure treated hydrothermally at 393 K, and (d) at 423 K for 1 day. It is evident that CdS nanoparticles with particle sizes less than 20 nm are well attached and dispersed on the surface of micrometer-size $AgGaS_2$. From this TEM image, it was

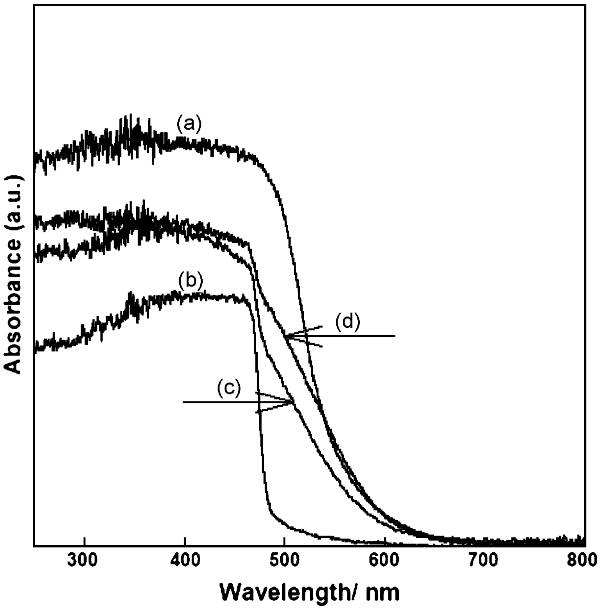

Fig. 8. UV–vis diffuse reflectance spectra (a) CdS treated hydrothermally at 393 K for 1 day, (b) AGS treated under H_2S/He flow at 1123 K for 3 h, (c) CdS/AGS PCD treated hydrothermally at 393 K for 1 day, and (d) CdS/AGS PCD treated hydrothermally at 423 K for 1 day.

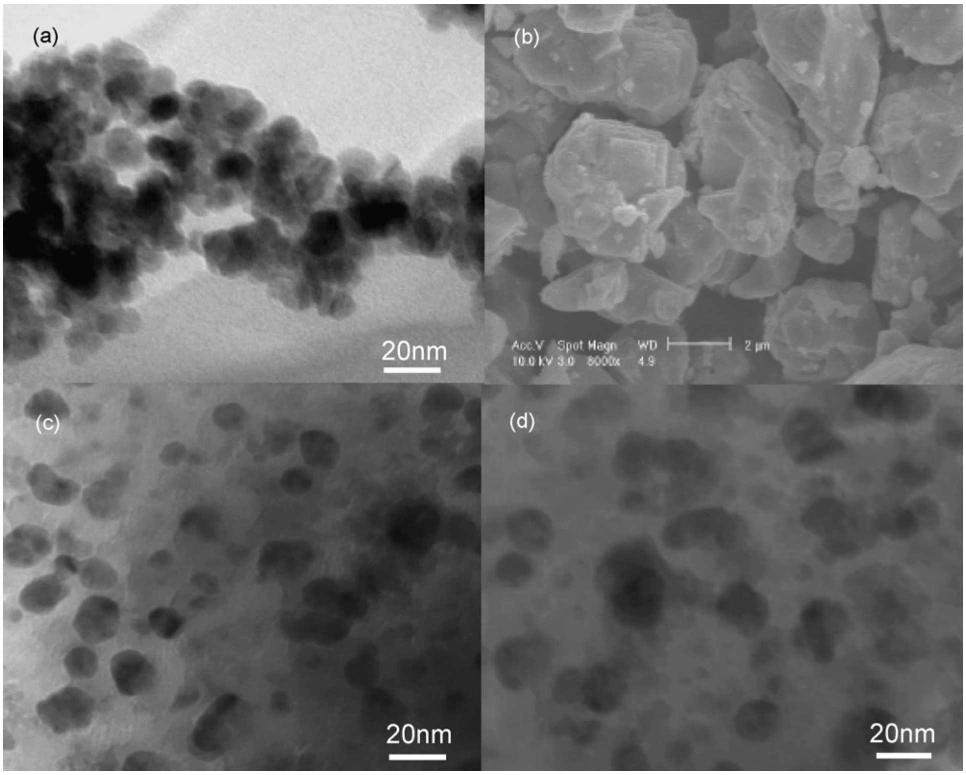

Fig. 9. TEM and SEM images of (a) CdS treated hydrothermally at 393 K for 1 day, (b) AGS treated under H_2S flow at 1123 K for 3 h, (c) CdS/AGS PCD treated hydrothermally at 393 K for 1 day, (d) CdS/AGS PCD treated hydrothermally at 423 K for 1 day, and (e) 1 wt.% Pt deposited on CdS/AGS PCD treated hydrothermally at 423 K for 1 day.

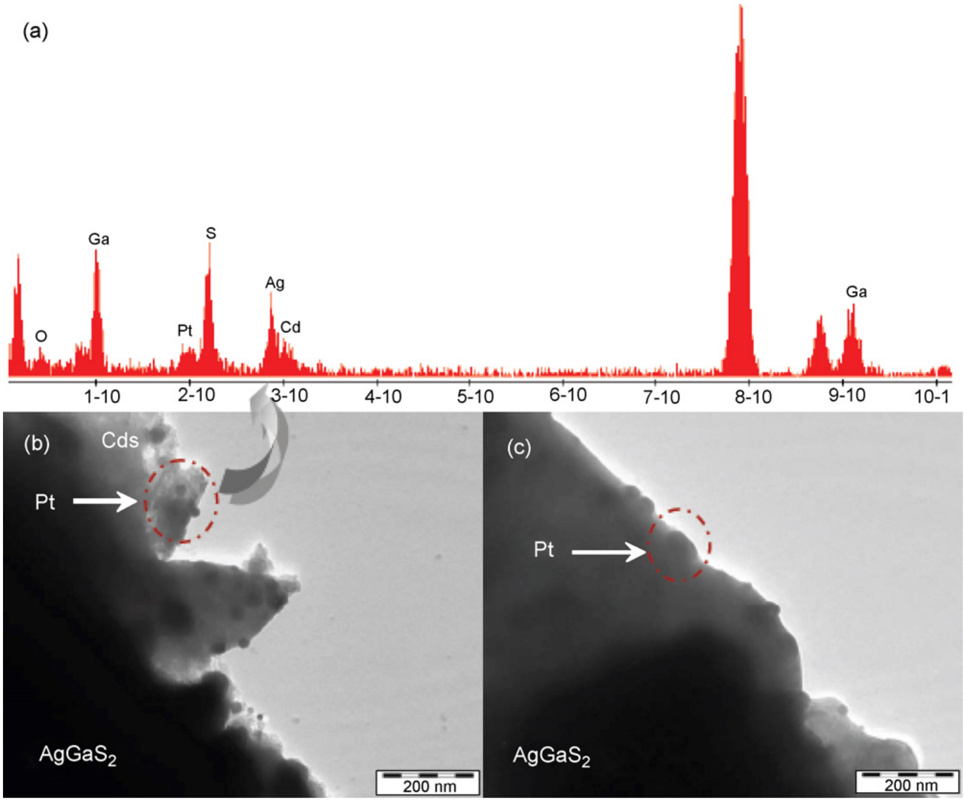

Fig. 10. EDAX data (a) and TEM images (b and c) of 1 wt.% Pt-loaded CdS/AGS PCD. The CdS/AGS PCD was prepared by hydrothermal treatment at 423 K for 1 day.

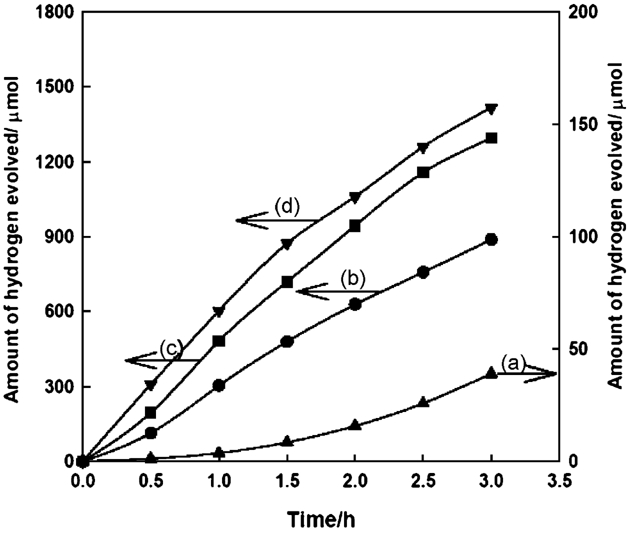

Fig. 11. Photocatalytic hydrogen production at room temperature over (a) CdS treated hydrothermally at 393 K for 1 day, (b) AGS treated under H_2S flow at 1123 K for 3 h, (c) CdS/AGS PCD treated hydrothermally at 393K for 1 day, and (d) CdS/AGS PCD treated hydrothermally at 423 K for 1 day. All samples were heat-treated under H_2S/He flow for 3 h before the reaction. Catalysts: 0.1 g loaded with 1 wt.% Pt, electrolyte: 0.1 M Na_2S + 0.02 M Na_2SO_3.

confirmed that fabrication of nano-bulk composite structure was successfully accomplished with the hydrothermal treatment method. The morphology change of CdS with different temperatures of hydrothermal treatment was observed by TEM analysis. CdS in untreated CdS/AGS composite did not show a clear shape of particles (not shown). But, as the temperature of hydrothermal treatment increased, CdS clearly showed nanosized particles of 20–30 nm (Fig. 9c and d) as nano-islands attached and dispersed on the surface of p-type semiconductor ($AgGaS_2$). To investigate where the Pt cocatalyst is loaded, we analyzed EDAX and TEM images. From EDAX (Fig. 10a) data and TEM images (Fig. 10b and c), we confirmed that 1 wt.% Pt-loaded CdS/AGS PCD consisted of Pt, CdS, and $AgGaS_2$, and that Pt cocatalysts were randomly loaded both on CdS and AGS particles of the CdS/AGS composite.

Shown in Fig. 11 are the results of photocatalytic hydrogen production from aqueous electrolyte solution containing 0.1 M Na_2S and 0.02 M Na_2SO_3 as sacrificial reagents under visible light irradiation (using a cut-off filter of $\lambda \geq 420$ nm for all catalysts). The rate of hydrogen production over photocatalytic diode (PCD) of CdS/$AgGaS_2$ was higher than the sum of single-component $AgGaS_2$ and CdS photocatalysts having similar crystallinity. The p-type material $AgGaS_2$ shows a H_2 evolution rate of 296 μmol h^{-1}. The p–n diode photocatalyst CdS/AGS shows a higher activity with the rate of 432 μmol H_2 h^{-1}. Note that nanosized CdS photocatalyst produces only small amount of H_2 (13 μmol h^{-1}). When CdS/AGS photocatalyst was hydrothermally treated at a higher temperature of 423 K, the rate of hydrogen production increased to 473 μmol h^{-1}. It means that the fabrication condition of CdS/AGS photocatalytic diode is important for hydrogen production although they did not show significant difference in XRD patterns and UV diffuse reflectance spectra of CdS/AGS samples. The rates observed for $AgGaS_2$ and CdS/AGS (H.T. at 423 K for 1day) photocatalysts, both loaded with 1 wt.% Pt, represent ca. 12.4 and 19.7% of the quantum yields (100 × the number of hydrogen atoms produced/number of absorbed photons) at $\lambda \geq 420$ nm, respectively.

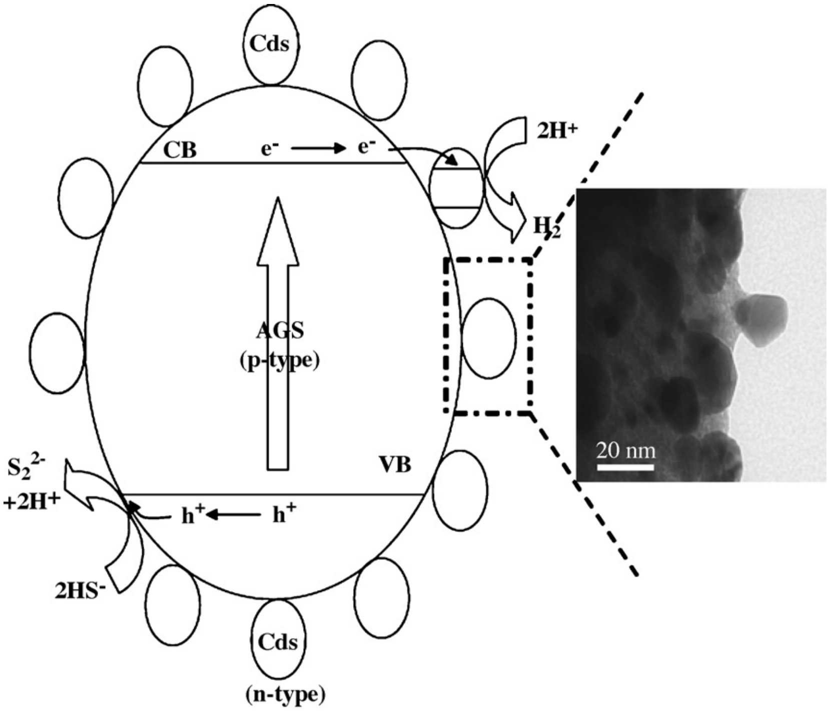

Fig. 12. A configuration model consisting of bulky AGS, p-type semiconductor with high crystallinity decorated with nanosized CdS particles, n-type semiconductor. Inset shows the TEM image that supports this structure model.

Based on the presented data, it can be concluded that the proposed fabrication of p–n composite semiconductors can be a successful and generic strategy to develop highly active photocatalysts under visible light. As discussed, $AgGaS_2$ can be made as a low-resistivity p-type semiconductor, but n-type conductivity appears difficult or impossible to achieve [11–14]. In contrast, CdS can be made as n-type, but not as p-type [15,16]. The fundamental direct band gap energy of wurtzite CdS is 2.42 eV at 300 K, close to that of $AgGaS_2$ (2.68 eV). Consequently, comparable injection ratios are likely for electrons and holes if they form a CdS/AGS diode structure. Schematic of its structure model (together with a TEM image that supports the structure) is shown in Fig. 12. The synergy observed for the p–n diode system may be attributable to efficient charge separation, caused by the rectification that sends photo-electrons and holes generated toward the opposite directions as indicated in Fig. 12. Thereby, the chance of electron-hole recombination is greatly reduced. This leads to high quantum yields and high photocatalytic activity of hydrogen production under visible light irradiation.

4. Conclusions

Bulky $AgGaS_2$ (AGS) photocatalysts were heat-treated at high temperatures under H_2S gas flow and the crystallinity and purity of the material was further improved. AGS heat-treated at high temperatures (1073–1123 K) showed a high photocatalytic activity for hydrogen production from electrolyte solution containing sulfide and sulfite as sacrificial reagents under visible right irradiation ($\lambda \geq 420$ nm). The non-oxide typed photocatalytic diode n-CdS/p-$AgGaS_2$ was successfully fabricated by hydrothermal treatment. The diode system formed with the n- and p-type semiconductors results in efficient charge separation, caused by the rectification of photo-electrons and holes generated. This results in the reduction of energy-wasteful electron-hole recombination and high photocatalytic activity of hydrogen production under visible light irradiation.

Acknowledgments

This work was supported by the National Research Laboratory Program, General Motors R&D Center.

References

[1] S.A. Naman, M. Grätzel, J. Photochem. Photobiol. A: Chem. 77 (1994) 249.
[2] C.A. Linkous, T.E. Mingo, N.Z. Muradov, Int. J. Hydrogen Energy 19 (1994) 203.
[3] A.B. Ellis, S.W. Kaiser, M.S. Wrighton, J. Am. Chem. Soc. 98 (1976) 6855.
[4] I. Tsuji, H. Kato, H. Kobayashi, A. Kudo, J. Am. Chem. Soc. 126 (2004) 13407.
[5] H.G. Kim, D.W. Hwang, J.S. Lee, J. Am. Chem. Soc. 126 (2004) 8912.
[6] P.W. Yu, Y.S. Park, J. Appl. Phys. 45 (1974) 823.
[7] P.W. Yu, Y.S. Park, J. Appl. Phys. 45 (1974) 3694.
[8] L. Brus, Appl. Phys. A 53 (1991) 465.
[9] J.L. Shay, B. Tell, H.M. Kasper, Appl. Phys. Lett. 19 (1971) 366.
[10] I. Choi, S. Eom, P.Y. Yu, J. Appl. Phys. 37 (2000) 3815.
[11] S. Wagner, J.L. Shay, B. Tell, H.M. Kasper, Appl. Phys. Lett. 22 (1973) 351.
[12] S. Kobayashi, Y. Momiyama, F. Kaneko, Jpn. J. Appl. Phys. 30 (1991) 1747.
[13] S. Wagner, J. Appl. Phys. 45 (1974) 246.
[14] M. Balkanski, R.D. Waldron, Phys. Rev. 12 (1958) 123.
[15] D.W. Niles, D. Rioux, H. Hochst, J. Appl. Phys. 73 (1993) 4586.
[16] M. Matsumura, S. Furukawa, Y. Saho, H. Tsubomura, J. Phys. Chem. 89 (1985) 1327.
[17] O. Khaselev, J. Turner, Science 280 (1998) 425.
[18] H.G. Kim, H.B. Pramod, J.S. Lee, Angew. Chem. Int. Ed. 44 (2005) 4585.
[19] A.J. Nojik, Appl. Phys. Lett. 29 (1976) 150;
A.J. Nojik, Appl. Phys. Lett. 30 (1977) 567.
[20] JCPDS cards, 27-615.
[21] N. Yamamoto, K. Yokota, H. Horinaka, J. Cryst. Growth 99 (1990) 747.
[22] J.S. Jang, W. Li, S.H. Oh, J.S. Lee, Chem. Phys. Lett. 425 (2006) 278.
[23] H. Weib, A. Fernandez, H. Kisch, Angew. Chem. Int. Ed. 40 (2001) 3825.
[24] H. Kisch, H. Weib, Adv. Funct. Mater. 12 (2002) 483.
[25] J. Rodriguez-Carvajal, Collected Abstracts of Powder Diffraction Meeting, Toolouse, France, 1990.